A New Capability for Measuring Dynamic Air Loads in a Wind Tunnel

IRVING C. STATLER,* ORREN B. TUFTS,† AND WALTER J. HIRTREITER‡
Cornell Aeronautical Laboratory Inc., Buffalo, N. Y.

This paper reviews the capabilities provided by the Cornell Aeronautical Laboratory's new system for dynamic testing in wind tunnels. By means of this unique mounting system, a model can be forced precisely in any desired planar sinusoidal motion. A series of wind-tunnel tests with this facility permitted, for the first time, the measurement of the separate components of the rotary damping moment. The moment due to rate of change of angle of attack was measured by oscillating the model in pure plunging motion. The moment due to pitch rate was measured during pitching motion. The sum of these is compared with the total rotary damping moment as measured in rotation. Comparisons of data taken at two frequencies and four Mach numbers indicate that the components are accurate to within ±10% of the total rotary damping moment. The results are compared with theory, flight-test data, and other wind-tunnel measurements on the same and similar models. Future applications of this equipment are reviewed, particularly with regard to its use as a research tool to support basic investigations for the development of theoretical or semiempirical methods for predicting dynamic-stability characteristics of aircraft at transonic speeds.

Introduction

THE diversity of operation and the unusual configurations of present-day aircraft introduce new problems in prediction of flight stability and control. The designer who must know the dynamic-stability characteristics of a new aircraft configuration to predict its handling qualities when it flies at high subsonic and transonic speeds faces a dilemma, however. Available theories for predicting the required aerodynamic characteristics in this speed range are totally inadequate. There are, currently, no proven methods for predicting the unsteady aerodynamic loads at transonic speeds and at the low reduced frequencies typical of aircraft rigid-body dynamics. To aid in the development of such a theory and to advance the technical understanding of unsteady transonic flow in general, there exists a requirement for wind-tunnel tests of unsteady aerodynamics in the transonic speed range. In recognition of this need, Cornell Aeronautical Laboratory Inc. (CAL), under sponsorship of the U. S. Air Force Research and Technology Division, Flight Dynamics Laboratory, Control Criteria Branch, undertook the development of a unique oscillatory mounting system by means of which a model in a wind tunnel can be forced precisely in any desired planar sinusoidal motion. Longitudinal short-period dynamic testing was chosen for the initial program to limit the equipment and experimentation necessary for obtaining useful and correlative results. The methods and equipment are, nevertheless, applicable to lateral dynamic testing as well.

The dynamic measurement of aerodynamic stability derivatives in wind tunnels is not a new undertaking. A review of some of the early techniques is given by B. Melville Jones in Ref. 1. Reviews of more recent literature on dynamic wind-tunnel testing[2–15] show that some of the basic techniques developed in those first years of aviation are still used today. These recent reports contain descriptions of current oscillators, instrumentation, and model-building practices. They represent curved flow or nonoscillatory testing techniques, free-oscillation methods, resonant excitation systems, a variety of inexorable forcing techniques, and two new free-flight approaches[11,12] but, generally, they are limited to considerations of the measurement of total damping.

The unique capabilities provided by the CAL/Air Force Dynamic Testing System result from the ability to inexorably force the model in any desired planar sinusoidal motion. In particular, three basic motions can be achieved to study longitudinal dynamics. These are:

1) A pure rotational motion about the model's center of gravity. Both the angle of attack and the pitch angle vary continuously, as in the flight path shown in Fig. 1a. The translational velocity is zero and the angle of attack equals the rotational angle. Dynamic measurements can be made of the lift and pitching moment due to angle of attack ($F_\alpha\boldsymbol{\alpha}$ and $M_\alpha\boldsymbol{\alpha}$) and also of the total rotary (dynamic) forces, which are composed of the sum of the contributions due to rate of change of angle of attack and the contributions due rate of rotation $[(F_{\dot\alpha} + F_{\dot\theta})\dot{\boldsymbol{\theta}}$ and $(M_{\dot\alpha} + M_{\dot\theta})\dot{\boldsymbol{\theta}}]$.

2) A pure plunging or translatory motion. The angle of attack varies continuously but is due only to the translational velocity, since there is no significant rotation about the model's center of gravity, as in the flight path shown in Fig. 1b. Dynamic measurements again can be made of the lift and moment due to angle of attack as in rotation but, more important, the lift and moment due to rate of change of angle of attack alone (i.e., $F_{\dot\alpha}\dot{\boldsymbol{\alpha}}$ and $M_{\dot\alpha}\dot{\boldsymbol{\alpha}}$) can be evaluated.

3) A pure pitching motion. This is the particular combination of rotational and translational motion such that the angle of attack remains constant, as shown in the flight path of Fig. 1c. In general, the effective oscillatory angle of attack of the model is the vector sum of the oscillating rotational angle about the c.g., $\boldsymbol{\theta}$, and the angle of attack due to the translational velocity of the c.g., $\mathbf{z}/U$, i.e., $\boldsymbol{\alpha} = \boldsymbol{\theta} + \dot{\mathbf{z}}/U$. The oscillating rotational angle is equal in amplitude and opposite in phase to the angle of attack due to the plunging motion. Thus, the net angle of attack is maintained constant in pure pitching motion. This motion permits measuring the lift and moment due only to rotational (or pitch) rate (i.e., $F_{\dot\theta}\dot{\boldsymbol{\theta}}$ and $M_{\dot\theta}\dot{\boldsymbol{\theta}}$). Similar considerations pertain to directional-lateral dynamics when the model is rotated by 90° on the balance support.

Presented as Paper 66-15 at the AIAA 3rd Aerospace Sciences Meeting, New York, N. Y., January 24–26, 1966; submitted February 4, 1966; revision received May 12, 1966. Work performed for U.S. Air Force Flight Dynamics Laboratory, Contract AF33-(616)-8034.

* Head, Applied Mechanics Department. Member AIAA.
† Principal Engineer, Applied Mechanics Department. Member AIAA.
‡ Principal Engineer, Applied Mechanics Department.

Dynamic-Testing System

The basic components of the dynamic-testing system are represented in Fig. 2. The operator adjusts the controls on the mechanical oscillator so that the model is forced into a desired planar sinusoidal motion. The motion is measured by linear and angular accelerometers in the model whereas forces and moments are measured by a strain-beam balance system between the model and the sting support. Signals from these transducers are passed through a signal-processing system that provides d.c. outputs proportional to the amplitudes and phases of the components of the force, moment, and accelerations at the oscillator frequency. This information, plus the oscillator frequency and tunnel test conditions, is displayed visually in the dynamic-testing control room (Fig. 3) and is recorded automatically and simultaneously in digital form

The dynamic balance and mechanical oscillator system was designed for use with CAL's 8-ft transonic variable-density wind tunnel. This wind tunnel is particularly well suited to the requirements of the system. Over a Mach number range of 0.50 to 1.20, dynamic pressures can be held constant in a range of 200 through 600 lb/ft^2, or Reynolds number/ft of reference length can be held constant at values of 1×10^6 through 3.5×10^6. Impact temperatures are held between 120° and 155°F, even for the supersonic speeds. This tunnel's 8-× 8-ft test section has perforated walls that permit complete performance measurements on models through the transonic speed range.

Mechanical Oscillator

The sting support for the model constitutes one arm of the linkage system (see Fig. 2) which is driven by connecting rods mounted eccentrically on two flywheels. Periodic motion at even low frequencies is assured by the large flywheel inertias.

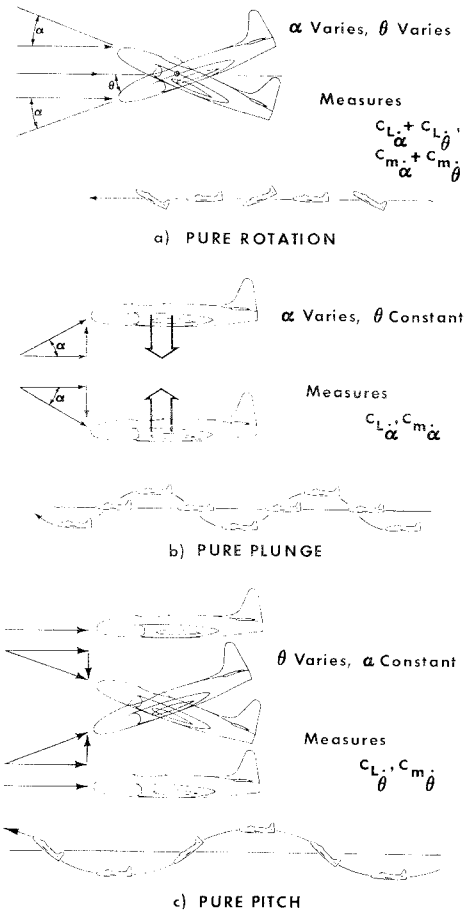

Fig. 1 Longitudinal motions of the model.

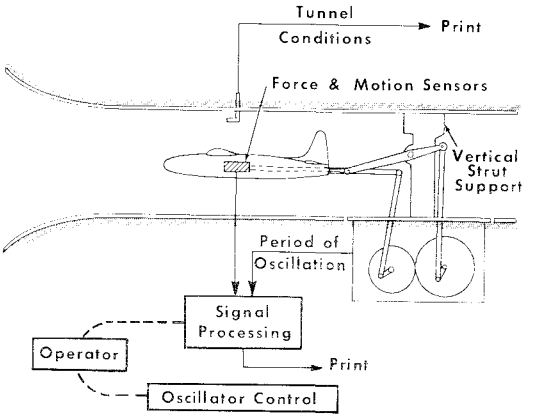

Fig. 2 Basic elements of the dynamic-testing system.

The desired model motion is obtained by adjusting the eccentric amplitudes and the angular relation between the flywheels. The eccentric amplitudes each are controlled by means of small hydraulic motors that are mounted on the flywheels. Each motor drives a drum, the periphery of which goes through the center of the flywheel, and the axis of which is parallel to that of the flywheel. A stub shaft on the drum completes the crank of the crank-connecting rod design. The eccentric drum is mounted on tapered roller bearings which reduce radial play to a minimum, even during amplitude adjustment. An annular hydraulic brake locks the drum, except while an eccentric adjustment is being made.

Control over the phase relationship between the two flywheels is obtained by means of a hydraulic motor which permits arbitrary angular positioning between the drive gear and shaft on the aft flywheel. Again, a hydraulically actuated brake locks these in position, except while adjustment is being made.

Indications of the forward and aft eccentric amplitudes and the phase between them are used by the operator initially to set up the desired motion approximately. The relationship between these measurements and the motion of the model can be computed beforehand on the assumption that the linkage system motion can be described by rigid-body kinematics. The final precise adjustments of the motion are made, however, on the basis of the indicated linear and angular accelerations of the model itself. This enables ob-

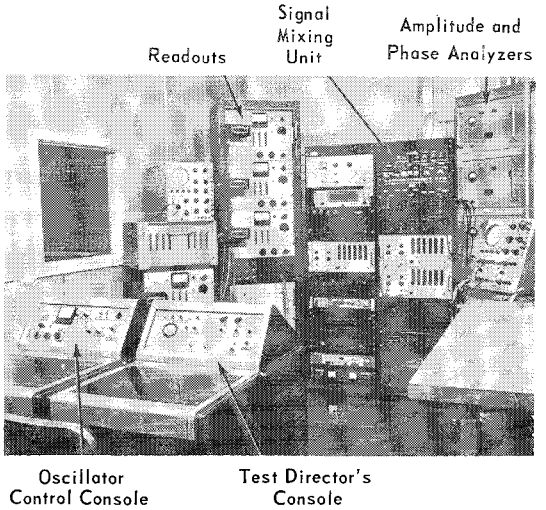

Fig. 3 Dynamic-testing control room.

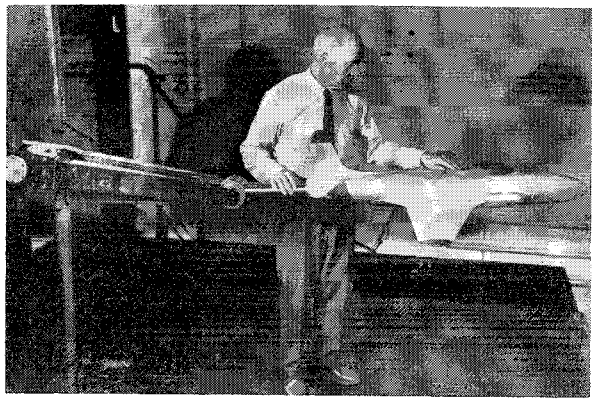

Fig. 4 Dynamic-testing model.

tainment of the desired model motion irrespective of the elastic distortions of the support system.

Although the mechanical details of their operation are rather complicated, the actual controls provided to the operator are very simple. On/off switches and a variable resistance potentiometer provide the control for the oscillator driving motor. The amplitudes of the forward and aft eccentrics can be increased or decreased at either a fast or slow speed. Another variable resistance potentiometer controls the rate of phase adjustment, and an on/off switch activates the phase control at this preset rate.

The dynamic loads produced by the oscillator in its own support structure are attenuated by mounting the oscillator on a large mass (14 tons, in fact) which, in turn, is isolated from the wind-tunnel structure by a pneumatic suspension. The very low resonance frequency of this mount system practically eliminates the transmission of any dynamic loads to the tunnel structure and, at the same time, isolates the model from random vibrations produced by the tunnel itself.

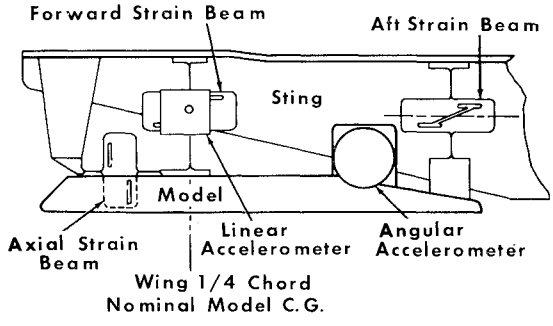

a) Schematic

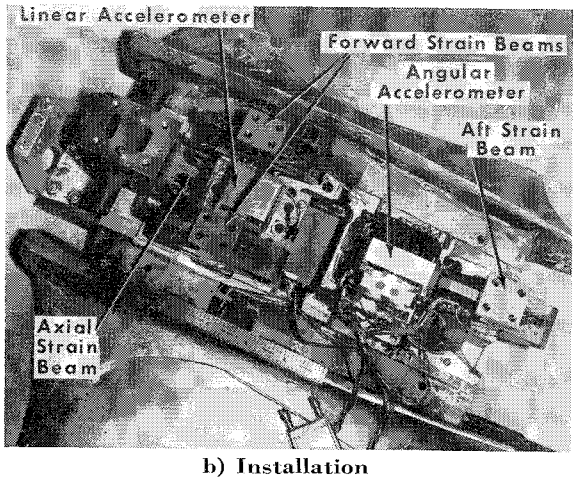

b) Installation

Fig. 5 The force and motion sensors.

The mechanical oscillator has the following operating characteristics: 1) it can provide a fundamental oscillating frequency of from 3–12 cps; 2) at this fundamental frequency, it can provide a translational motion of up to 20 g's of translational acceleration or a vertical displacement of 1-ft double amplitude; 3) it can provide a rotational motion of the model at the fundamental frequency with angular accelerations in excess of 200 rad/sec^2, or a rotational displacement of 10° double amplitude; and 4) the system can sustain a peak vertical load of 1200 lb at the model's center of gravity.

Model

For purposes of checkout, shakedown, and evaluation of this dynamic-testing system, a $\frac{1}{10}$-scale model of an F-80 aircraft was utilized (shown in photo of Fig. 4). Although it is not a particularly modern design, this F-80 model was used in these tests because of the relatively large amount of comparable data available from other wind-tunnel tests, calculations, and flight tests. This light, rigid, and strong model was built specifically to make dynamic wind-tunnel tests for comparison with full-scale flight-test data. The weight and moment of inertia of the model were kept small to minimize the inertial loads on the balance. The model is, however, very rigid to avoid introducing effects due to aeroelastic deformations of the model. (For details on the model design and construction, see Ref. 13.)

Force and Motion Sensors

The measurement system in the model is shown in the sketch of Figure 5a and in the photograph of Fig. 5b. The model is supported from the sting by a system of four flexures, three of which incorporate strain gages for the generation of needed data signals. The strain gages on two of these flexures, the forward strain beams, are connected to sum their output signals. This signal is, henceforth, referred to as the normal-force measure although, actually, it includes a component proportional to the pitching moment. The model is balanced precisely so that its center of gravity is located longitudinally at the sensitive axes of the forward strain beams, which are located as closely as possible to the aerodynamic center of the model (in this case, the quarter chord of the wing). A single flexure support is situated aft of the forward flexures and on the model's longitudinal centerline. The strain-gage bridge attached to this flexure provides output proportional to pitching moment only. A fourth flexure called the axial strain beam is attached between the model and sting to provide restraint along the longitudinal axis without interfering with the operation of the sensing flexures.

The vertical motion at the model's center of gravity is measured by a modified Model 4310 Linear Accelerometer manufactured by the Donner Scientific Company. The standard 4310 Accelerometer consisting of seismic element and associated electronics is housed in a single case that is too large to fit the space available at the center of gravity of the model. The modified unit obtained for this purpose consists of two parts, a sensing element housed in a small case, and an electronic components package in a separate case. The sensing element is located at the model's center of gravity and the electronic package is in the vertical strut. This accelerometer has a full-scale range of ±30 g's. Under all operational environments existing during wind-tunnel testing, the instrument exhibits an over-all accuracy of 1% or better.

The model's rotary motion about a pitching axis is measured by means of a Unico Controls Inc. Model MCA-6 Angular Accelerometer. This instrument was developed especially for the dynamic-testing system and it is unique in its small size, ruggedness, insensitivity to inputs other than angular acceleration, and its attenuation of high-frequency noise

inputs. The inertial sensing element in this transducer is designed for minimum mass unbalance. If it were not the case, prohibitively large errors would result from the instrument's response to linear accelerations when attempting to measure small angular accelerations during model motions which included large linear accelerations (plunge and pitch). This angular accelerometer has a full-scale range in excess of ± 200 rad/sec^2. Its sensitivity to linear acceleration, measured under 15-g conditions, is an output signal at 1 g that is less than that equivalent to ± 0.05 rad/sec^2 of angular acceleration input. The transducer signals from the model are processed on line to provide digitized readouts of the amplitudes and phases of the forces, moments, and accelerations at the oscillation frequency.

Signal Processing

A block diagram of the signal-processing system is shown in Fig. 6. The signal-processing system simultaneously accepts the four transducer outputs originating in the model at a particular frequency within the range of 3–12 cps, extracts the fundamental signals in the presence of random noise and harmonic frequencies, and automatically derives from these signals their phase angles and individual magnitudes. This information is displayed visually and is printed out and punched on IBM cards for later use in performing the final analysis.

The four signals from the force and motion transducers in the model are fed to a signal-mixing unit. The operations performed in the signal amplification and mixing unit are shown in Fig. 7. Phase-compensation controls (padders) are provided in the linear acceleration, force, and moment channels to accommodate differences in dynamic characteristics of the transducers and to match these channels dynamically at each frequency to the angular accelerometer channel. These signals then can be combined as desired. In particular, the forces and moments due to inertial reactions are compensated by corresponding signals of opposite polarity from the linear and angular accelerometers.

The four signals from the mixing unit are then fed to four phase and amplitude analyzers that incorporate unique filtering capabilities. These units were also developed especially for this system by Unico Controls Inc. Each unit automatically supplies, first, an output in digital form proportional to the phase angle with respect to the oscillator of the part of the signal which is at the fundamental oscillator frequency and, second, an output voltage proportional to the amplitude of the fundamental component of the signal from the model transducer. This filter system is self-synchronous with respect to the fundamental input frequency, so that harmonics or random noise in the input signal are strongly attenuated regardless of the frequency of the fundamental signal. Consequently, the two outputs from each channel are very accurate digitized measures of the amplitude and the phase of the fundamental, sinusoidal component of a noisy input signal.

System Accuracy Requirements

The acceptable tolerances in the measured derivatives were arbitrarily selected to be the following in order to establish the accuracy objectives for the system: 1) The error in F_α shall be less than 10% of F_α. 2) The error in M_α shall be less than 10% of M_α. 3) The error in $M_{\dot\alpha} + M_{\dot\theta}$ shall be less than 10% of $M_{\dot\alpha} + M_{\dot\theta}$. 4) The error in $M_{\dot\alpha}$ shall be less than 10% of $M_{\dot\alpha} + M_{\dot\theta}$. 5) The error in $M_{\dot\theta}$ shall be less than 10% of $M_{\dot\alpha} + M_{\dot\theta}$.

Requirements on the system accuracy fall into two categories: One is the requirement on the accuracy with which the desired motion must be set up, and the other is the requirement on the accuracy with which that motion and the resulting force and moment must then be measured. In the first category, the very precise control on the oscillator, together with the accurate on-line readouts of the model accelerations, enables the operator to adjust the model motion within extremely tight tolerances. For example, the control is sufficiently precise to adjust the model motion at 7 cps to within ± 0.4 rad/sec^2 of rotational acceleration, to well within ± 8 ft/sec^2 of the plunging acceleration, and to about $\pm \frac{1}{2}°$ of phase angle between rotation and plunging. These represent the order of accuracy of motion required by the pure pitching case when it is desired to maintain the rate of change of angle of attack at less than about 0.03 rad/sec.

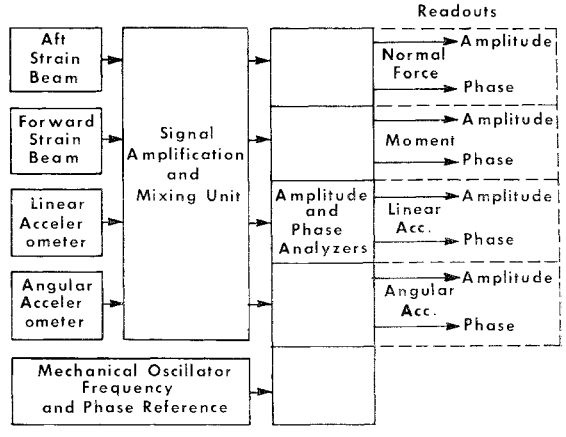

Fig. 6 Signal-processing system.

In the second category, every consideration has been given to maximizing the measurement accuracy of each element of the system. The transducers are designed to separate their functions clearly in order to tailor the sensitivity of each to the specific quantity to be measured. The model motions are also tailored to the particular measurement to be made. Ideally, with an errorless measuring system, the motion of the model could be arbitrary. Since this perfection cannot be achieved, specific motions, such as pitching, plunging, and rotation in the case of longitudinal dynamics, are used to maximize particular components of the loads to be measured. This use of a particular motion for each measurement maximizes the accuracy possible within the resolution limitations of the data processing system. In much the same way, readout accuracy is improved by canceling, in the mixing unit, the components of force and moment due to inertial loads.

System Evaluation Tests

Just prior to the wind-on tests, a program of wind-off tests was performed to set up the desired gains, adjust the phase paddings on the signal channels, and combine the signals in the proper proportions in accordance with Fig. 7. In wind-off pure rotation tests, a signal from the angular accelerometer was combined in the mixing unit with the signal from the

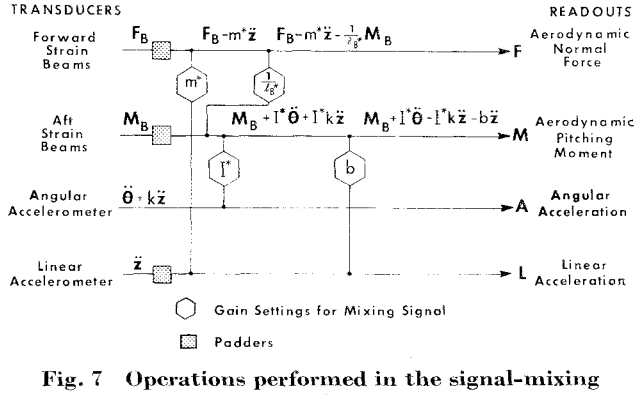

Fig. 7 Operations performed in the signal-mixing unit.

moment balance, and a gain (I^* in Fig. 7) was adjusted until the moment readout was zero. The moment due to inertial reaction thus was canceled.

In wind-off pure plunging tests, a signal from the linear accelerometer was combined in the mixing unit with the signal from the moment balance, and the gain (b in Fig. 7) was adjusted to reduce the component of the moment in phase with linear acceleration to zero. (For the F-80, there was a residual moment due to the drag load on the horizontal tail which led the linear acceleration by 90° and was about 0.5 ft-lb at 7 cps and 15 g's of linear acceleration in a $\frac{1}{2}$-atm environment.) A signal from the linear accelerometer was combined with the signal from the normal-force beams in the mixing unit, and the gain (m^* in Fig. 7) was adjusted to minimize the normal-force readout. A signal from the moment balance was combined in the mixing unit with the signal from the forward (normal-force) beams, and the gain ($1/l_B{}^*$ in Fig. 7) was adjusted to zero the normal-force readout. This compensated for the component of moment sensed by the forward beams.

The system was then ready for wind-on tests. A series of wind-tunnel tests using the F-80 model at three frequencies and four Mach numbers demonstrated the versatility and over-all accuracy of the dynamic-testing system. The tests were run in the following order, all at densities corresponding to $\frac{1}{2}$ atm at wind-off.

1) Pure rotation tests were run at 50 rad/sec^2 with less than $\frac{1}{4}$ g of linear acceleration. The frequency was 7 cps. Data were taken at Mach numbers 0, 0.5, 0.7, 0.75, 0.8, and repeated at M = 0.

2) Pure plunging tests were run at 15 g's of linear acceleration and less than 0.4 rad/sec^2 of angular acceleration. Again, the frequency was 7 cps and the Mach numbers were 0, 0.5, 0.7, 0.75, 0.8, and repeated at M = 0.

3) Pure pitching tests were performed at 15 g's of linear acceleration at a frequency of 7 cps. The motion was adjusted so that the phase of the angular acceleration lagged the linear acceleration by 90° ± $\frac{1}{2}$°. In all cases, the linear acceleration was adjusted to 15 g's ± $\frac{1}{4}$ of a g, and the angular acceleration required at each Mach number was adjusted to within ±0.4 rad/sec^2. At M = 0.5 (U = 550 fps), the required angular acceleration to cancel the angle of attack due to 15 g's of translational motion at 7 cps is 38.6 rad/sec^2. At M = 0.7 (U = 767 fps), the angular acceleration is 27.7 rad/sec^2. At M = 0.75 (U = 824 fps), the angular acceleration is 25.8 rad/sec^2, and at M = 0.8 (U = 882 fps), the angular acceleration is 24.1 rads/sec^2. The entire test program was then repeated at a frequency of 5 cps, and the pure rotation tests were also conducted at 10 cps.

A major consideration during the development of the dynamic-testing system was the necessity for a sufficiently strong fundamental signal that would not be lost in the noise environment caused by random vibration and aerodynamic turbulence. These tests demonstrated that a very high signal-to-noise ratio was indeed maintained. This is due, in large part, to the high g levels that can be obtained, the firmness of the model-motion system, the isolation mounting of the mechanical oscillator, and the over-all design of the instrumentation and signal-processing system.

Data Reduction and Analyses

The data which were automatically printed out during these tests were analyzed in accordance with the equations developed in the following discussion: $\mathbf{F_B}$ is the reactive force of the model on the normal-force strain beams defined as positive up, $\mathbf{M_B}$ is the reactive moment of the model on the aft strain beam defined as positive for model-nose-up, $\ddot{\mathbf{z}}$ is the linear acceleration of the model defined as positive down, and $\ddot{\boldsymbol{\theta}}$ is the angular acceleration of the model defined as positive for model-nose-up. In the most general case, the loads carried by the forward and aft strain beams are, respectively,

$$\left.\begin{aligned}\mathbf{F_B} &= m\ddot{\mathbf{z}} + (1/l_B)\mathbf{M_B} + F_\alpha\boldsymbol{\theta} + F_{\dot\theta}\dot{\boldsymbol{\theta}} + F_{\dot\alpha}\dot{\boldsymbol{\theta}} + F_\alpha(\dot{\mathbf{z}}/U) + F_{\dot\alpha}(\ddot{\mathbf{z}}/U)\\ \mathbf{M_B} &= -I\ddot{\boldsymbol{\theta}} + mx_{c.g.}\ddot{\mathbf{z}} + M_\alpha\boldsymbol{\theta} + M_{\dot\theta}\dot{\boldsymbol{\theta}} + M_{\dot\alpha}\dot{\boldsymbol{\theta}} + M_\alpha(\dot{\mathbf{z}}/U) + M_{\dot\alpha}(\ddot{\mathbf{z}}/U)\end{aligned}\right\} \quad (1)$$

where m is the mass of the model plus metric part of the balance (including the linear and angular accelerometers), l_B is the distance between the forward and aft strain beams, I is the moment of inertia of the mass m about its c.g., and $x_{c.g.}$ is the longitudinal displacement of the sensitive axis of the forward strain beams from the center of gravity of the mass m (positive aft). All the remaining terms on the right-hand side of Eqs. (1) are due to aerodynamic loads. In accordance with the operations performed in the mixing unit, as shown in Fig. 7, the aerodynamic normal-force and pitching moment are related to the balance measurements as follows:

$$\begin{aligned}\mathbf{F} &= \mathbf{F_B} - m^*\ddot{\mathbf{z}} - 1/l_B{}^*\,\mathbf{M_B}\\ \mathbf{M} &= \mathbf{M_B} + I^*\ddot{\boldsymbol{\theta}} + I^*k\ddot{\mathbf{z}} - b\ddot{\mathbf{z}}\end{aligned} \quad (2)$$

where m^* is used to cancel the normal force due to inertial reaction, $1/l_B{}^*$ is used to cancel the component of moment sensed by the forward strain beams, I^* is used to cancel the moment due to inertial reaction, k is the crosstalk sensitivity of the angular accelerometer, and b is used to correct for the effects of the crosstalk k and the c.g. location error $x_{c.g.}$. In terms of the actual readout indications, the model motion is expressed as (see Fig. 7)

$$\ddot{\mathbf{z}} = \mathbf{L} \qquad \ddot{\boldsymbol{\theta}} = \mathbf{A} - k\mathbf{L} \quad (3)$$

and for sinusoidal motion

$$\begin{aligned}\boldsymbol{\theta} &= -(\tau/2\pi)^2\ddot{\boldsymbol{\theta}} \qquad \dot{\boldsymbol{\theta}} = (\tau/2\pi j)\ddot{\boldsymbol{\theta}}\\ \dot{\mathbf{z}} &= (\tau/2\pi j)\ddot{\mathbf{z}}\end{aligned} \quad (4)$$

Equations (1–4) are combined to give

$$\left.\begin{aligned}\mathbf{F} = {} & \left\{-F_\alpha\left(\frac{\tau}{2\pi}\right)^2 + F_{\dot\theta}\left(\frac{\tau}{2\pi j}\right) + F_{\dot\alpha}\left(\frac{\tau}{2\pi j}\right)\right\}\mathbf{A} + \left\{\frac{1}{l_B} - \frac{1}{l_B{}^*}\right\}\mathbf{M_B} + \left\{U(m - m^*) + F_\alpha k\left(\frac{\tau}{2\pi}\right)^2 \times U - F_{\dot\theta}k\left(\frac{\tau}{2\pi j}\right)U - F_{\dot\alpha}k\left(\frac{\tau}{2\pi j}\right)U + F_\alpha\left(\frac{\tau}{2\pi j}\right) + F_{\dot\alpha}\right\}\frac{\mathbf{L}}{U}\\ \mathbf{M} = {} & \left\{I^* - I - M_\alpha\left(\frac{\tau}{2\pi}\right)^2 + M_{\dot\theta}\left(\frac{\tau}{2\pi j}\right) + M_{\dot\alpha}\left(\frac{\tau}{2\pi j}\right)\right\}\mathbf{A} + \left\{IkU + mx_{c.g.}U - bU + M_\alpha k\left(\frac{\tau}{2\pi}\right)^2 U - M_{\dot\theta}k\left(\frac{\tau}{2\pi j}\right)U - M_{\dot\alpha}k\left(\frac{\tau}{2\pi j}\right)U + M_\alpha\left(\frac{\tau}{2\pi j}\right) + M_{\dot\alpha}\right\}\frac{\mathbf{L}}{U}\end{aligned}\right\} \quad (5)$$

For wind-off tests, Eqs. (5) reduce to

$$\left.\begin{aligned}\mathbf{F} &= (m - m^*)\mathbf{L} + \left(\frac{1}{l_B} - \frac{1}{l_B{}^*}\right) \times [-I\mathbf{A} + (mx_{c.g.} + Ik)\mathbf{L}]\\ \mathbf{M} &= (I^* - I)\mathbf{A} + (mx_{c.g.} + Ik - b)\mathbf{L} + \mathbf{M_{TD}}\end{aligned}\right\} \quad (6)$$

where $\mathbf{M_{TD}}$ is the moment due to the drag load on the hori-

zontal tail during motion with no wind. The corresponding normal forces were neglected.

During the wind-off plunge tests, the gain m^* was adjusted to minimize the normal-force readout, and then the gain $1/l_B{}^*$ was adjusted to reduce this readout to zero. Hence, for wind-off conditions, the first of Eqs. (6) is $\mathbf{F} = 0$. The gain b was adjusted to make the quantity $mx_{c.g.} + I^*k - b$ equal to zero. Further, in wind-off pure rotation tests, the gain I^* was adjusted until the moment readout was zero. Hence, for wind-off conditions, the second of Eqs. (6) is $\mathbf{M} = \mathbf{M_{TD}}$.

Accordingly, the appropriate forms of Eqs. (5) for reducing the wind-on test data are the following:

Pure rotation

$$\mathbf{F} = \{F_\alpha(\tau/2\pi j) + (F_{\dot\alpha} + F_{\dot\theta})\}\tau\mathbf{A}/2\pi j$$

$$\mathbf{M} = \{M_\alpha(\tau/2\pi j) + (M_{\dot\alpha} + M_{\dot\theta})\}\tau\mathbf{A}/2\pi j$$

Pure plunge

$$\mathbf{F} = \left\{F_{\dot\alpha} + F_\alpha\left(\frac{\tau}{2\pi}\right)^2 kU + [F_\alpha - (F_{\dot\alpha} + F_{\dot\theta})kU]\left(\frac{\tau}{2\pi j}\right)\right\}\frac{\mathbf{L}}{U}$$

$$\mathbf{M} = \left\{M_{\dot\alpha} + M_\alpha\left(\frac{\tau}{2\pi}\right)^2 kU + [M_\alpha - (M_{\dot\alpha} + M_{\dot\theta})kU]\left(\frac{\tau}{2\pi j}\right)\right\}\frac{\mathbf{L}}{U}$$

The crosstalk sensitivity of the angular accelerometer k was sufficiently small so that negligible error was introduced when $F_\alpha(\tau/2\pi)^2kU$ was neglected with respect to $F_{\dot\alpha}$; $(F_{\dot\alpha} + F_{\dot\theta})kU$ was neglected with respect to F_α; $M_\alpha(\tau/2\pi)^2kU$ was neglected with respect to $M_{\dot\alpha}$; and $(M_{\dot\alpha} + M_{\dot\theta})kU$ was neglected with respect to M_α. Then

$$\mathbf{F} \cong \{F_{\dot\alpha} + F_\alpha(\tau/2\pi j)\}\mathbf{L}/U$$

$$\mathbf{M} \cong \{M_{\dot\alpha} + M_\alpha(\tau/2\pi j)\}\mathbf{L}/U$$

Pure pitch

$$\mathbf{F} = F_{\dot\theta}\left(\frac{\tau}{2\pi j}\right)\mathbf{A} + \left\{F_\alpha\left(\frac{\tau}{2\pi j}\right) + F_{\dot\alpha}\right\}\left(\frac{\tau\mathbf{A}}{2\pi j} + \frac{\mathbf{L}}{U}\right) + \left\{F_\alpha\left(\frac{\tau}{2\pi}\right)^2 - (F_{\dot\alpha} + F_{\dot\theta})\left(\frac{\tau}{2\pi j}\right)\right\}(kU)\frac{\mathbf{L}}{U}$$

Table 1 Lift derivatives

	5 cps		7 cps		10 cps	
M	$C_{L\dot\alpha} + C_{L\dot\theta}$	$C_{L\alpha}$	$C_{L\dot\alpha} + C_{L\dot\theta}$	$C_{L\alpha}$	$C_{L\dot\alpha} + C_{L\dot\theta}$	$C_{L\alpha}$
			Rotation			
0.5	34.2	5.31	6.1	5.17	17.8	4.77
0.7	34.8	5.84	−3.9	5.67	4.1	4.2
0.75	35.4	5.85	−4.0	5.84	7.3	5.1
0.8	34.9	4.77	2.6	4.70	...	...
			Plunge			
	$C_{L\dot\alpha}$	$C_{L\alpha}$	$C_{L\dot\alpha}$	$C_{L\alpha}$	$C_{L\dot\alpha}$	$C_{L\alpha}$
0.5	...	5.30	39.1	5.08	...	...
0.7	...	5.66	44.3	6.10	...	...
0.75	...	5.59	52.1	6.49	...	...
0.8	...	4.64	47.6	4.97	...	...
			Pitch			
	$C_{L\dot\theta}$	...	$C_{L\dot\theta}$	...	$C_{L\dot\theta}$	...
0.5	...	...	1.6	[0.3]	...	...
0.7	...	...	−17.6	[0.6]	...	...
0.75	...	...	−16.4	[0.6]	...	...
0.8	...	...	11.9	[0.4]	...	...

Table 2 Moment derivatives

	5 cps		7 cps		10 cps	
M	$C_{m\dot\alpha} + C_{m\dot\theta}$	$C_{m\alpha}$	$C_{m\dot\alpha} + C_{m\dot\theta}$	$C_{m\alpha}$	$C_{m\dot\alpha} + C_{m\dot\theta}$	$C_{m\alpha}$
			Rotation			
0.5	−13.2	−0.38	−13.0	−0.36	−12.8	−0.39
0.7	−12.8	−0.28	−13.1	−0.30	−13.0	−0.35
0.75	−13.7	−0.31	−13.6	−0.31	−13.7	−0.37
0.8	−14.7	−0.23	−14.3	−0.24	...	...
			Plunge			
	$C_{m\dot\alpha}$	$C_{m\alpha}$	$C_{m\dot\alpha}$	$C_{m\alpha}$	$C_{m\dot\alpha}$	$C_{m\dot\alpha}$
0.5	−5.0	−0.38	−3.4	−0.38	...	...
0.7	+0.2	−0.45	−0.2	−0.42	...	...
0.75	−1.2	−0.42	−1.9	−0.42	...	...
0.8	−3.9	−0.34	−2.3	−0.31	...	...
			Pitch			
	$C_{m\dot\theta}$	...	$C_{m\dot\theta}$	...	$C_{m\dot\theta}$	...
0.5	−10.3	[0.01]	−10.9	[0.00]	...	...
0.7	−13.4	[0.00]	−11.4	[0.00]	...	...
0.75	−13.4	[0.01]	−11.5	[0.00]	...	...
0.8	−14.2	[0.01]	−12.7	[0.01]	...	...

$$\mathbf{M} = M_{\dot\theta}\left(\frac{\tau}{2\pi j}\right)\mathbf{A} + \left\{M_\alpha\left(\frac{\tau}{2\pi j}\right) + M_{\dot\alpha}\right\}\left(\frac{\tau\mathbf{A}}{2\pi j} + \frac{\mathbf{L}}{U}\right) + \left\{M_\alpha\left(\frac{\tau}{2\pi}\right)^2 - (M_{\dot\alpha} + M_{\dot\theta})\left(\frac{\tau}{2\pi j}\right)\right\}(kU)\frac{\mathbf{L}}{U}$$

If the pitching motion has been set up accurately, then $\boldsymbol{\theta} = -\dot{\mathbf{z}}/U$ or, in terms of the readouts $(\tau\mathbf{A}/2\pi j) + \mathbf{L}/U$ is approximately (except for the crosstalk effect) equal to zero in this case. The second term in each of the preceding equations can then be neglected. In all of the tests of pitch motion, this term was found to be well within the allowable error. Further, the value of k is sufficiently small to make the third term negligible, so that for pure pitch

$$\mathbf{F} \cong F_{\dot\theta}(\tau\mathbf{A}/2\pi j) \qquad \mathbf{M} \cong M_{\dot\theta}(\tau\mathbf{A}/2\pi j)$$

The preceding resolution of the force and moment vectors into their components in phase and in quadrature with the relevant motion in each of the three cases permits the evaluation of the lift and moment derivatives.

The results for the lift derivatives and moment derivatives for the F-80 model obtained during these dynamic wind-tunnel tests are presented in Tables 1 and 2. The measurements of $C_{L\alpha}$ at 5 and 7 cps from rotation and from plunge are in good agreement. They are, furthermore, in good agreement with the general band of data covered by calculated, flight-test and static wind-tunnel data[14,16] as shown in Fig. 8.

In the case of the moments, the dynamic measurements of $C_{m\alpha}$ at 5, 7, and 10 cps from rotation are in excellent agree-

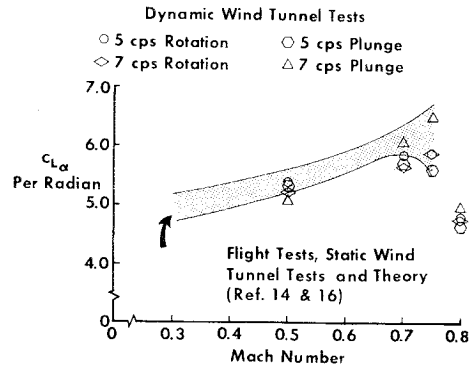

Fig. 8 Lift curve slope vs Mach number.

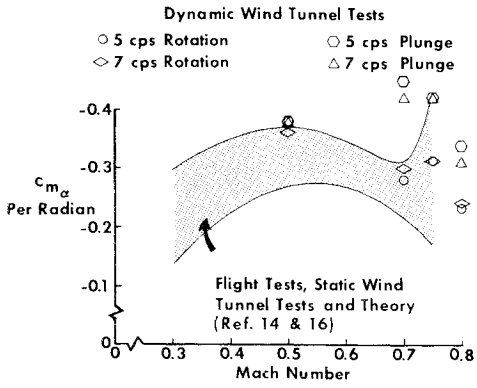

Fig. 9 Moment curve slope vs Mach number.

ment. This agreement demonstrates the repeatability of the test data, since these tests were completely independent; in fact, they were performed on different days. The C_{m_α} values from these dynamic measurements are in good agreement with the band covered by flight-test data and calculations as shown in Fig. 9. The dynamic measurements of C_{m_α} from plunge tests at 5 and 7 cps are also in good agreement with each other, but there are significant differences between the rotation and the plunge results in the region of Mach 0.7 to 0.8. The amplitudes of the oscillatory angle of attack during the rotation tests were about double those achieved in plunge at the highest speeds. The differences are attributed to the nonlinearity of the moment curve with angle of attack for the F-80 at high Mach numbers.

Finally, the total rotary damping derivative vs Mach number showing the band of reference data and the measurements from rotation tests are presented in Fig. 10. Again, note the agreement of measurements at 5 and 7 cps. These data points also compare favorably with the total derivative as determined from the sum of plunge and pitch measurements, and all data points lie well within the band of reference data. The measured values of the rotary lift derivatives, $C_{L_{\dot\alpha}} + C_{L_{\dot\theta}}$, presented in Table 1 are obviously too inaccurate to be meaningful. Table 2 shows that the values for $C_{m_{\dot\alpha}}$ from plunge at 5 and 7 cps compare well at each Mach number, as do the values for $C_{m_{\dot\theta}}$ from pitch at 5 and 7 cps.

Recall that the objective of established accuracy with this system was the ability to measure $C_{m_{\dot\alpha}}$ and $C_{m_{\dot\theta}}$ each to within $\pm 10\%$ of their sum as measured in pure rotation. This, then, means that the sum of $C_{m_{\dot\alpha}}$ from plunge and $C_{m_{\dot\theta}}$ from pitch should be within $\pm 20\%$ of $(C_{m_{\dot\alpha}} + C_{m_{\dot\theta}})$ as measured in rotation. In all cases but one, this objective has been achieved very adequately. In the one exceptional case (5 cps at M = 0.8), the error in the sum is 23%.

There appears to be a sufficiently large sample of experimental evidence to verify that the objectives of over-all accuracy for the dynamic-testing system have been achieved. The capabilities of the dynamic-testing system have been demonstrated by these measurements of the longitudinal aerodynamic derivatives of the F-80 model. For further details of this program, see Ref. 17.

Future Applications of the Dynamic-Testing System

Since the F-80 model was limited to subsonic speeds because of buffeting, additional investigations were performed with a more advanced model through transonic speeds. The similar test program conducted with an F-104 model at speeds up to M = 1.2 achieved a comparable degree of success. The results are reported in Ref. 18.

The additional capabilities built into the present equipment are noteworthy, although there are no plans for their immediate use. All tests to date have been performed with the model at a mean angle of attack close to that for trim. The static angle of attack of the model can be adjusted, however, so that the model can be oscillated about various values of mean angle of attack. Also, lateral dynamic tests, similar to the longitudinal experiments, could be carried out by rotating the model 90° on the balance support.

The system now can be used in routine dynamic wind-tunnel tests comparable to current static wind-tunnel testing programs. These will provide a body of reference data to aid in estimating the dynamic-stability characteristics and handling qualities of other new designs. Apart from such design studies, dynamic wind-tunnel tests will be used for the purpose of checking the validity of theoretical calculations in those cases where appropriate theories are available. Most significantly, however, the dynamic-testing system will be used for basic research studies to advance the understanding of unsteady transonic flow in general. The objective of this research will be to aid the development of a proven adequate analytical technique for predicting the unsteady aerodynamic loads at transonic speeds, and at the low reduced frequencies typical of aircraft rigid-body dynamics.

The dynamic-testing system is being prepared currently for use in a program, the objective of which is to determine the validity of available methods for predicting unsteady pressures in transonic flow by comparison with experimental results. Measurements will be made of the unsteady pressures at the surface of an inexorably oscillated rigid-wing model, as well as of the integrated aerodynamic forces and moments on the model produced by this motion. These results, along with flow visualization, will then provide the bases for verification of available theoretical methods. The model to be tested is a 70°-delta, single-wedge configuration. Twenty-six pressure transducers are to be installed in the model. Wind-tunnel tests will be performed at several combinations of Mach number and Reynolds number, while the model is oscillated at various discrete frequencies in rotation, plunge, and pitch. This program is a joint effort by CAL and North American Aviation Inc. and is cosponsored by the Aerospace Dynamics Branch and the Control Criteria Branch of the Air Force Flight Dynamics Laboratory.

In attempting to formulate a theory for transonic unsteady aerodynamic predictions, experimental data will be used not only to evaluate available theories but to inspire new developments as well. A definitive program of research is required to provide experimental data accurate enough to be useful in further development of techniques for predicting transonic unsteady aerodynamic loads. The objectives of such a program are served most effectively by utilizing the CAL/Air Force Dynamic-Testing System. This facility, with its specialized signal-processing and readout equipment, provides a unique capability for dynamic measurements in a wind tunnel which is ideally suited to the requirements of such a research program. It offers, for the first time, an opportunity for prescribed variations of motion content, that is, rotation and translation, and for a systematic investigation of effects of frequency, Mach number, Reynolds

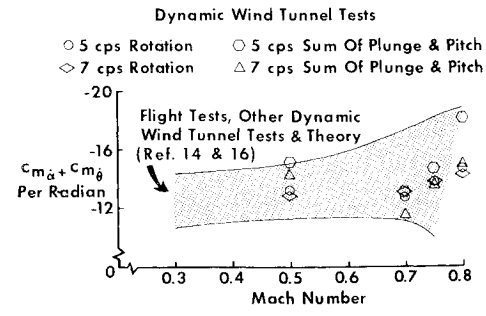

Fig. 10 Rotary damping derivative vs Mach number.

number, and configuration parameters on the fundamental constituents of longitudinal and lateral dynamic stability characteristics at transonic speeds.

References

[1] Durand, W. F., "Dynamics of the airplane," *Aerodynamic Theory* (Dover Publications, New York, 1963), Vol. V, Div. N, (first published by Julius Springer, Berlin, 1935).

[2] Valensi, J., "A review of the techniques of measuring oscillatory aerodynamic forces and moments on models oscillating in wind tunnels in use on the continent," AGARD paper AG15 P6, Fifth Meeting of the Wind Tunnel and Model Testing Panel (May 1954).

[3] Arnold, L., "Dynamic measurements in wind tunnels," AGARDograph 11 (August 1955).

[4] Beam, B. H., "A wind-tunnel test technique for measuring the dynamic rotary stability derivatives at subsonic and supersonic speeds," NACA Rept. 1258 (1956).

[5] Welsh, C. J. and Clemens, P. L., "A small-scale forced-oscillation dynamic balance system," Arnold Engineering Development Center TN58-12, Armed Services Technical Information Agency AD-157143 (July 1958).

[6] Orlik-Ruchemann, K., "Methods for measurement of aircraft dynamic stability derivatives," National Research Council of Canada, Aeronautical Rept. LR-254 (July 1959).

[7] Scherer, M. and Mathe, P., "Measurement of aerodynamic derivatives in the wind tunnel and in flight," AGARD Meeting (April 1961).

[8] Scherer, M., "Mésure des derivées aerodynamiques en ecoulement transsonique et supersonique," Office National d'Etudes et de Recherches Aerospatiales Publ. 104 (1962).

[9] Braslow, A. L., Wiley, H. G., and Lee, C. Q., "A rigidly forced oscillation system for measuring dynamic-stability parameters in transonic and supersonic wind tunnels," NASA TN D-1231 (March 1962).

[10] Vaucheret, X., "Determination of the dynamic stability derivatives by the method of free oscillations," Office National d'Etudes et de Recherches Aerospatiales Publ. 20 (1963).

[11] Reed, W. H., III and Abbott, F. J., Jr. "A new 'free-flight' mount system for high speed wind tunnel flutter models," Proceedings of Symposium on Aeroelastic and Dynamic Modeling Technology, RTD-TDR-63-4197, Pt. I (March 1964).

[12] Hill, J. A. and Gikas, X. A., "Application of aeroelastic modeling techniques to the determination of structural loads and stability and control dynamic characteristics," Proceedings of Symposium on Acroelastic and Dynamic Modeling Technology, RTD-TDR-63-4197, Pt. I (March 1964).

[13] Tufts, O. B., Duryea, G. R., Jr., MacArthur, R. C., and Zimmerman, A. H., "Longitudinal airplane dynamics wind tunnel testing equipment," Wright Air Development Center TR-55-184 (July 1955).

[14] Tufts, O. B. and MacArthur, R. C., "Measurement of dynamic stability derivatives in the wind tunnel—Part I: Development testing of the apparatus," Wright Air Development Center TR-57-274, Pt. I, Armed Services Technical Information Agency AD-118258 (April 1957).

[15] Daughaday, H., DuWaldt, F., and Statler, I., "Measurement of dynamic stability derivatives in the wind tunnel—Part II: Evaluation of testing techniques," Wright Air Development Center TR-57-274, Pt. II, Armed Services Technical Information Agency AD-118258 (May 1957).

[16] Kidder, R. C., "Dynamic longitudinal stability flight tests of an F-80A airplane by the forced oscillation and step function response methods including measured horizontal tail loads," Cornell Aeronautical Lab. Rept. TB-495-F-11 (February 1950).

[17] Statler, I. C., Tufts, O. B., and Hirtreiter, W. J., "The development and evaluation of the CAL/Air Force dynamic wind-tunnel testing system, Part I—description and dynamic tests of an F-80 model," Air Force Flight Dynamics Lab. TR 65-153, Part I (September 1966).

[18] Statler, I. C., "The development and evaluation of the CAL/Air Force dynamic wind-tunnel testing system, Part II—dynamic tests of an F-104 model," Air Force Flight Dynamics Lab. TR-65-153 (October 1966, Part II).